LA-UR-01-5310
Approved for public release;
distribution is unlimited.

Title: **PROGRESS TOWARD UNDERSTANDING MAGNETIZED TARGET FUSION (MTF)**

Author(s): R.C. Kirkpatrick, I.R. Lindemuth, D.C. Barnes, R.J, Faehl, P.T. Sheehey, C.E, Knapp

Submitted to:

PROGRESS TOWARD UNDERSTANDING MAGNETIZED TARGET FUSION (MTF)

R.C. Kirkpatrick, I.R. Lindemuth, D.C. Barnes,
R.J, Faehl, P.T. Sheehey, C.E, Knapp

Los Alamos National Laboratory
Los Alamos, New Mexico 87545, USA

ABSTRACT

Magnetized target fusion (MTF) takes advantage of 1) the reduction of the electron thermal conductivity in a plasma due to magnetization and 2) the efficient heating through bulk compression. MTF proposes to create a warm plasma with an embedded magnetic field and to compress it using an imploded liner or shell. The minimum energy required for fusion in an optimized target is directly proportional to the mass of the ignited fusion fuel. Simple theoretical arguments and parameter studies have demonstrated that MTF has the potential for significantly reducing the power and intensity of a target driver needed to achieve fusion. In order to acquire a comprehensive understanding of MTF and its potential applications it is prudent to develop more complete and reliable computational techniques. This paper briefly reviews the progress toward that goal.

1. INTRODUCTION

In terms of operating density magnetic-confinement fusion energy (MFE) and inertial confinement fusion (ICF) are extreme approaches to controlled fusion, with as much as twelve orders of magnitude separation in operating density. MTF operates in an intermediate density range between the two extremes, approximately six orders of magnitude higher than MFE and a few orders of magnitude below ICF. This is possible because MTF takes advantage of cross-field reduction of electron thermal conduction by a magnetic field and the efficient heating possible by near-adiabatic compression. A two-step process is employed. It is necessary to first create a warm, magnetized plasma, and then to compress it to fusion temperatures. The warm plasma must have a temperature in excess of about 50 eV to provide sufficient electrical conductivity to trap an embedded field in excess of about 50 kG, and the compression must heat it to over 5 keV.

Only a few MTF experiments have been carried out during the quarter century since magnetized targets were first considered for fusion energy applications, and thus far the meager results continue to be encouraging. Therefore, the arguments for MTF have been largely based on theory. We have explored the parameter space for MTF and emphasized the potential benefits of its more modest driver requirements in the attainment of a practical fusion energy system. It is clear that a more vigorous pursuit of MTF is

Current Trends in International Fusion Research -- Proceedings of the Fourth Symposium
Edited by Charles D. Orth, Emilio Panarella, and Richard F. Post, NRC Research Press,
National Research Council of Canada, Ottawa, ON K1A 0R6 Canada, 2001.

merited, but to garner the necessary resources, it is essential to advance the general understanding of MTF beyond its present state.

2. EXAMPLES OF MAGNETIZED TARGETS

One of the earliest examples of an MTF target was the Sandia Phi-target, which will be discussed in more detail below. Other possible approaches to MTF are compression of a Z-pinch initiated plasma and the Russian MAGO experiment. In the Z-pinch target, a discharge is initiated in a frozen deuterium-tritium (DT) fiber on the axis of a closed cylindrical liner. The discharge creates the warm, magnetized plasma, after which the liner is compressed by a current along its periphery. Another approach, the MAGO experiment, appears to have produced a moderately dense plasma at about 200 eV [1], and if the MAGO plasma is determined to be sufficiently pure, it could be compressed to fusion temperatures with a slow liner that converges to about one-tenth of its original radius. Such compressions should not be difficult. Yet another example is represented by a field-reversed configuration (FRC) compressed by a cylindrical liner. In the remaining sections we discuss some experiments and calculations relating to the above examples.

3. SANDIA PHI TARGET

The Sandia Phi-target represents the most physically complete MTF experiment to date. The Phi-targets were created from plastic ICF microballoon targets used on one of the Sandia National Laboratory electron-beam (e-beam) machines. In the mid 1970s Sandia National Laboratory was imploding small microballoons with ReHyd, a 1 MeV relativistic pinched e-beam machine that was powered by a Marx capacitor bank with a coaxial water line used for pulse compression. This simple ICF target was mounted on a stalk on the anode of the e-beam machine. The current in the diode of the machine was sufficient to self-pinch the beam. Early experiments showed that the energy deposition was anomalously high, which was later determined to be due to reflexing of the relativistic electrons through the target. However, a non-relativistic early current (or prepulse) was also discovered, which tended to produce an asymmetric implosion. In order to eliminate the non-relativistic prepulse a very thin collector plate was added to the target on the cathode side. When the collector plate built up sufficient charge (and resultant voltage across the millimeter-sized microballoon), a discharge occurred inside the microballoon, which created a warm, slightly magnetized plasma. When the main relativistic current followed, the energy deposited by the relatively long-range relativistic electrons in the main pulse caused the thin microballoon to explode, driving its inner aspect inward and compressing the plasma and field together. Between 5 and 25 million neutrons were inferred from measurements for eight of the 15 complete targets. Each neutron burst occurred near the time of expected maximum compression during the operation of the target, but no neutrons were detected for any of the 24 null targets fielded to test other possible sources of neutrons. These were the first neutrons produced by e-beam implosion. Only limited diagnostics were fielded, and there was no direct compression measurement. A separate experiment indicated that the prepulse should create a 20 eV magnetized plasma. Detailed 2-D MHD calculations done later showed that the temperature should have reached 400 eV with a volumetric compression of about 8000, in order to provide the inferred thermonuclear neutron production [2]. The magnetic field probably reached 100 T near the time of maximum compression, but the magnetization parameter $\omega\tau$ (where ω is the electron cyclotron frequency and τ is the mean electron-electron collision time) was only about 5. These were remarkable results, considering the simplicity of the targets, the low implosion velocity, and the small amount of energy deposited in each target (about 4 kJ). Because magnetized targets were not expected to provide high gain (a requirement for success with laser-driven

fusion, but not pulsed power-driven fusion), they were abandoned in favor of unmagnetized targets. Later a computational study indicated that MTF target gains of about 100 might be possible for larger and more complex targets [3].

4. ENERGY BALANCE

For typical ICF targets, electron thermal conduction is the dominant energy loss mechanism during compression. A sufficiently strong magnetic field can significantly reduce electron thermal conduction loss if the density is low enough to provide a large enough magnetization parameter $\omega\tau$. Lower density also reduces free-free emission (i.e., bremsstrahlung) from the plasma. If a warm, magnetized plasma is compressed the values of density, temperature and magnetic field all increase. By focusing on the temperature rate equations and assuming that the electron and ion temperatures are the same in a homogeneous fusion fuel contained in a spherical shell, the net rate of temperature change depends on the work rate (-PdV/dt) due to compression, the fusion energy self-heating, the thermal conduction (both electron and ion), the bremsstrahlung (or free-free) emission, the inverse Compton cooling, the synchrotron radiation, and the re-radiation of the shell material. If a uniform azimuthal magnetic field (B_θ) is completely trapped inside the shell, it will increase inversely as the square of the radius (R^{-2}) of its confining shell. Therefore, B_θ should be proportional to the areal density (ρR). Simultaneous solution of the temperature rate equations and the equations for target radius and velocity, plasma density, etc. under the above simplifying assumptions, permit a quick survey of parameter space for magnetized target fusion (MTF). Such a survey revealed that there is a new region in the parameter space for thermonuclear fusion, which exists at lower initial density ρ_o and initial implosion velocity v_o [4] than necessary for ICF. These regions also correspond to very low driver power and intensity on target. The reduced driver requirements for MTF make compression by efficient electrical pulsed power schemes attractive. Most of the survey discussed in ref. 4 assumed that all the fusion energy escaped the target (a very conservative assumption that precluded fusion self-heating and ignition), but the possible impact of self-heating was considered.

5. FUSION IGNITION

For ICF, high target gain is dependent on fusion ignition, that is self-heating by deposition of the energy from the energetic reaction products overcoming the conduction plus radiative and expansion cooling in the burning fusion plasma. Because the drivers for MTF could potentially be much more efficient than for ICF, ignition and high gain may not be essential for the success of MTF, but ignition does lead to moderately high gain targets [3]. For ignition to occur, part of the fusion energy must be returned to heat the fusion fuel. The two most important parameters for self-heating are the areal density (ρR) and the field-times-radius parameter (BR) for the fusion fuel. The field configuration and gradients are of secondary importance. At the higher values of BR, the energy deposition is greater for the case of a uniform B_θ than for the case of a field with a linear gradient produced by a uniform Jz current density. Similar results are obtained for the case of a gradient due to a current concentrated on axis. This is demonstrated in Figure 1.

In order to magnetically insulate the fusion fuel using readily achievable internal magnetic fields in the fusion target, it is necessary to operate with a lower fuel density than for ICF. Classical reduction of the cross-field electron thermal conductivity due to an electron $\omega\tau$ product of about 10 is about two orders of magnitude. Higher values of electron $\omega\tau$ are not useful because of the ion thermal conduction, which requires a higher magnetic field or operation at lower density for suppression. Operation at a lower fuel

density also reduces the bremsstrahlung radiation. However, because the density is much higher than for magnetically confined plasmas, in comparison with bremsstrahlung synchrotron radiation is not an important cooling mechanism [5]. Also, the fuel energy density is much greater than the magnetic field energy density, so that most of the compression work done goes into increasing the internal energy of the fusion fuel rather than the field energy. If the fuel is to be driven to fusion temperatures, the compression rate must be sufficient to overcome the reduced energy loss rates due to thermal conduction and radiation. Also, sufficiently high BR enhances the energy deposition by the fusion reaction products, which may lead to fusion ignition, in a manner similar to ignition in ICF.

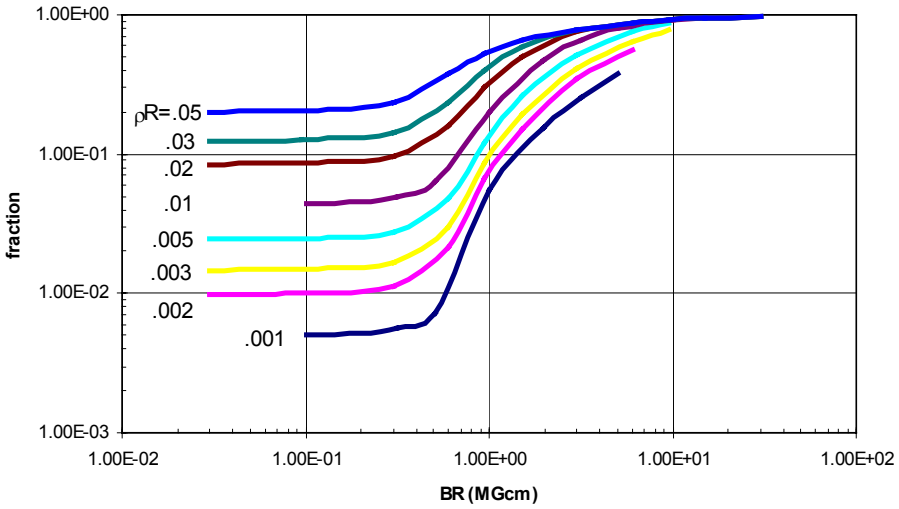

Figure 1. DT alpha particle energy deposited in spherical volume for the case of a current concentrated on the axis (B(r) = B(R)R/r).

The temperature rate equations (including self-heating due to DT alpha energy deposition from the fusion processes) define the boundary between two regions in the temperature-areal density (T-ρR) plane, one where the temperature increases and the other where the temperature decreases [6]. When the target is in the beginning stages of implosion, the work rate (-PdV/dt) dominates all other terms and the temperature increases, but as the plasma pressure grows, the imploding shell around the fusion fuel decelerates, and the various losses increase, so that eventually all the initial kinetic energy of the shell is converted into internal energy within the target and shell. Ideally, the velocity throughout the shell goes to zero, so that momentarily there is no compression heating, and at that moment all the energy in the target is in the form of internal energy. If at that moment the temperature is still increasing, fusion ignition has occurred. In the case of ICF where there is no magnetic field, fusion ignition cannot occur for $\rho R < 0.3$ g/cm^2 or a temperature below about 4.5 keV [6]. However, for MTF with sufficient magnetic field, as the target mass is increased, the region where fusion overcomes the various energy loss rates (when PdV/dt = 0) extends to values of ρR far below 0.3 g/cm^2. The extent of the MTF ignition region depends on both the target mass and magnetic field. For target masses below 10-100 micrograms and fields weaker than about 200 T, ignition cannot occur for MTF. The minimum T and ρR required for ignition define a minimum pressure times radius parameter <PR>, and the value of this minimum depends the target mass as well as the magnetic field.

6. MINIMUM ENERGY FOR IGNITION

Shortly after driver has ceased to operate, almost all the target energy is kinetic, mostly in the shell surrounding the fusion fuel. As the implosion proceeds, the internal energy in the fusion fuel and the target shell increase. In the absence of energy loss, conservation of energy together with an ignition criterion (minimum PR) lead to a simple relation for the minimum energy needed for ignition in an optimized target as a function of implosion velocity:

$$E = mc_vT\, v^2 / [v^2 - 2e_o\{<PR>^{3/2} / (mc_vT/2\pi)^{1/2}\}^a] \ ,$$

where <PR> is the minimum value that allows ignition, v is the initial implosion velocity, m is the mass of the fusion fuel, c_v is the specific heat, T is the fusion ignition temperature, e_o is related to the shell equation of state, $a = (\gamma-1)/\gamma$, and γ is the ratio of specific heats for the shell material. At the very least, the thermal energy in the fusion fuel mc_vT must be supplied, and for low implosion velocities, significantly more must be supplied. If the initial implosion velocity is too low, ignition becomes energetically impossible. The lower <PR>, the lower the value of v for ignition, and the lower the minimum energy required for ignition. Because <PR> depends on the mass m and the magnetic field, the relation has a more complicated behavior than is apparent in the simple relation above. However, since <PR> for MTF can be much less than one-tenth of that needed for ICF, the implosion velocity needed to provide the requisite internal energy for MTF ignition can be quite low.

The above result is based purely on energy balance, with no consideration of energy loss from the magnetized plasma into the surrounding shell during the implosion. The reduced energy loss rate from the magnetized plasma also plays role in determining the minimum implosion velocity for fusion ignition. The rate of energy transfer into the surrounding shell was only partially included through the rate equations used in the evaluation of the minimum <PR> required for ignition. The amount of internal energy transferred from the magnetized plasma into the surrounding shell during the compression process was not included in the <PR> evaluation. As the implosion velocity is reduced toward the minimum defined by the above equation this neglect becomes increasingly important, so a more complete analysis is needed. Of course, any complete numerical calculation would account for this energy transfer.

7. TARGET PLASMA

The price for reducing the driver requirements is the creation of a warm, magnetized target plasma suitable for subsequent compression to fusion conditions. According to an MTF survey study done several years ago [4], it appears that the target plasma must have at least 1) a temperature greater than 50 eV, 2) a magnetic field greater than 5 T, and 3) an initial density in the range 10^{-3} to 10^{-6} gm/cc. Also, the lifetime of the target plasma must significantly exceed the time required for compression. Some of the possible methods of producing the requisite target plasma include Russian MAGO gas discharge experiment, a high-density Z-pinch, a theta-pinch discharge (FRC), and dynamic plasma assembly (merging spheromaks).

8. MAGO EXPERIMENTS

The joint US/Russian MAGO ("magnetic compression") experiments represent a very energetic approach to producing a target plasma for MTF [7]. MAGO uses an explosively driven electrical pulsed power circuit that consists of an inductor charged initially with a

seed current from a capacitor. The seed current is amplified by geometrically deforming the inductor in order to reduce its inductance. The amplified seed current passes through a rod along the axis of a chamber separated into two parts by a central copper barrier, which defines the inner radius of an annular nozzle between the two parts (see Figure 2). The current returns along the outer cylindrical wall, thereby establishing a magnetic field in the neutral gas in the chambers, after which the inductor is shorted by using an explosively driven closing switch. As the explosive continues to deform the inductor, the current is further amplified to several megamps and then again switched into the copper or aluminum MAGO chamber by using an explosively driven opening switch. The sudden rise in voltage across the annular nozzle and across an insulator causes two successive electrical breakdowns. It should be noted that smaller chambers have been driven by a capacitor bank, so explosive pulsed power is not a prerequisite for these experiments.

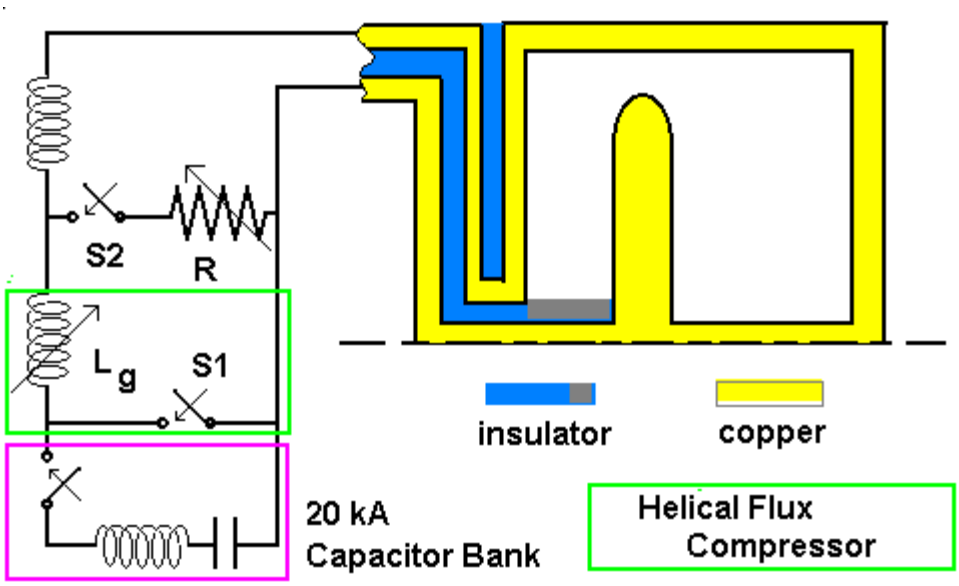

Figure 2. Typical MAGO experiment chamber and pulsed power circuit.

Los Alamos, Lawrence Livermore National Laboratory and the All-Russia Scientific Research Institute for Experimental Physics (VNIIEF) have performed detailed calculations of the MAGO chamber operation. The calculations indicate the initial breakdown occurs in the annular nozzle. A weaker breakdown occurs across the insulator in the first region and drives an inverse pinch, which forces the gas from the first region through the nozzle, where it is accelerated. The accelerated plasma shocks the gas in the second chamber and creates hot spots that give an initial burst of about 10^{13} neutrons. However, this transient, neutron producing plasma is not of particular interest. Continuing flow and relaxation bring the plasma in the second region to the desired target plasma conditions. After relaxation the bulk of the plasma in the second part of the chamber is warm and magneto-thermally insulated from the confining copper walls of the MAGO chamber.

To briefly summarize the above description of MAGO, a complex electrical discharge is used to drive a deuterium-tritium mixture inside a heavy copper chamber to about $10^{18}/cm^2$ particle density and about 200-300 eV in temperature. The early transient chamber operation gives an incidental burst of neutrons, but the cooler late-time quiescent

plasma is of more interest. If sufficiently pure (uncontaminated with hydrocarbons, copper, etc.), it may represent an ideal target plasma for MTF.

Our Russian colleagues have proposed various approaches for using an energetic, magnetically imploded solid liner to compress such a target plasma to fusion temperatures. If the MAGO target plasma is sufficiently clean, no facilities beyond the currently available explosive pulsed power facilities at VNIIEF in Russia should be needed for a convincing demonstration.

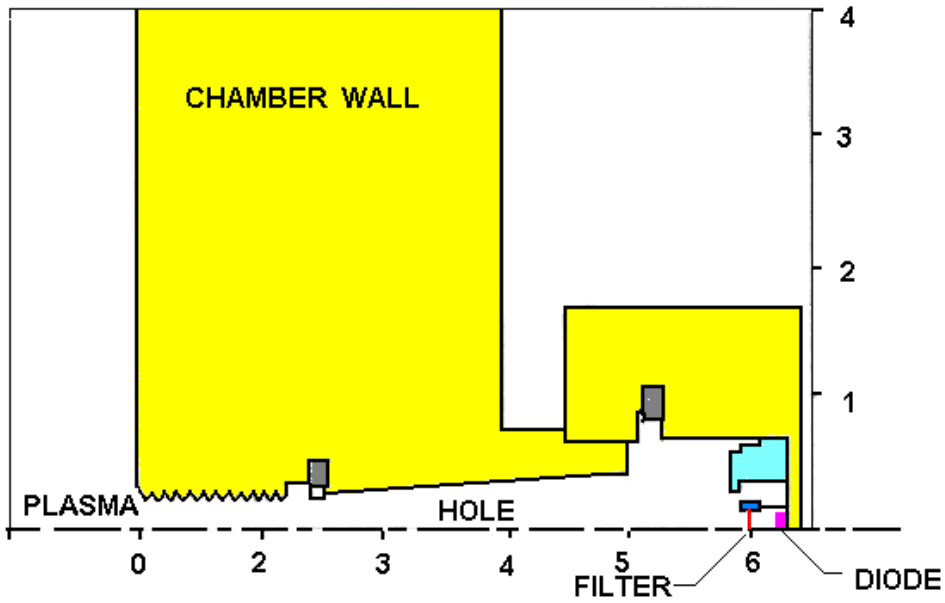

Figure 3. Configuration of a filtered silicon diode arrays for MAGO III. The Z coordinate is an axis of symmetry for the calculation.

9. MEASUREMENT OF THE MAGO PLASMA TEMPERATURE

Figure 3 shows the configuration for a filtered silicon diode array used in the 1995 MAGO III experiment in Russia. Holes were drilled through the copper chamber walls into the second region, and a tube was attached to each with filtered silicon diodes mounted at the end of the tube away from the chamber. The October 1994 MAGO II experiment used only one filtered silicon diode for each of several similar lines of sight into the chamber. For the first few microseconds after first breakdown, the signals for all diodes rose to a peak and then fell more slowly, but there followed an abrupt change in the character of the signals. The analysis [8] indicated an abrupt crash in temperature for the MAGO II experiment, but MAGO III could not be confidently analyzed.

Only a filter and low-density neutral gas in the access hole and connecting tube separated each diode from the plasma. The chamber and the connecting tubes all contained 10 torr of DT at the start of the experiment. According to 2-D MHD calculations, the operation of MAGO not only produces a warm plasma in the second part of the chamber, but the initially weak embedded magnetic field is compressed to higher flux density as well. This causes an imbalance in pressure between the DT gas in the tubes and the magnetized DT plasma in the chamber, so that a plasma piston should move into the hole.

The magnetized plasma in the second region of the MAGO chamber cannot travel freely into the diagnostic tubes because it is restrained by its embedded magnetic field. The geometry for the tube and its connection to the chamber is highly 3-D, but a simple picture

assumes that the field in the plasma is initially azimuthal (B_θ). When the pressure rises in the chamber, the plasma is pushed along with its embedded field into the tube. However, the plasma must do work to drag the field into the tube, because it is stretching the field in that part of the chamber. It is easy to derive a relation that describes the force acting to restrain the plasma's entry into the hole as a function of the distance traveled into the tube (or hole drilled in the side of he chamber). When the plasma has moved more than one radius into the tube, the restraining force ceases to increase.

If the pressure in the chamber is very high, then a very strong shock can travel into the tube, which would disrupt the filters very soon after operation began. If the plasma pressure is sufficiently low, then the plasma will travel only a short distance into the tube before being stopped by the embedded field. In such a case the plug of magnetized plasma will oscillate, driving successive weak shocks into the gas in the tube. The successive weak shocks merge in the tube, and the effect is to supply energy periodically at a relatively regular intervals to the head of the shock.

The shock speed is proportional to the average power that supports it. Based on our calculation of the average power, we were able to estimate the time required for the shock to reach the filters. For MAGO III only about 4 μs was required. Additional calculations indicated that the time required for the weak shock to rupture the filter after arrival at the filter was on the order of an additional microsecond. This analysis and auxiliary calculations indicated that there should be a delay of a few microseconds between the time of pressure rise in the chamber and filter disruption. This seems to explain the sudden change in the character of the filtered silicon diode signals that was observed in the data for both MAGO II and MAGO III. This is one example of how detailed analysis of the relevant physics processes can be a useful aid for fully understanding the experimental data.

We used the spectral characteristics of each diode folded with that of the diode in an analysis code to calculate each expected filtered diode response to a variety of spectral types, each characterized by a single parameter such as temperature or energy. Upon comparing the expected responses with the data, the closest match was selected for each time-dependent set of data. The five spectral types used were 1) bremsstrahlung, 2) Planck (e.g., black body) spectrum, 3) a spike at a given energy, 4) a flat spectrum out to a specified energy, and 5) an exponential characterized by a temperature. The basis for comparison was the diode response ratios. This way we created a history of the best matching temperature or energy for each of the spectral types [8].

Because theoretically the magnetized plasma spectrum should be closer to that of bremsstrahlung than to the other spectra, and an optically thick plasma radiating with a Planck spectrum as hot as that which matches the diode signal ratios would have a short lifetime indeed ($<< 1$ μs), we were forced to accept the bremsstrahlung or exponential histories as being the closest to the correct characterization of the MAGO II plasma. It appears that after initially rising to about 400 eV (rms) average temperature along the diode lines of sight, the electron temperature of the plasma fell somewhat below 200 eV and then slowly decreases with a lifetime significantly exceeding 4 μs, probably more than 10 μs. The abrupt crash in all temperatures corresponds to a sudden rise in all diode signals shortly after 8 μs. It appears that the sudden rise in signal corresponds to shock disruption of the filters just in front of the diodes, as discussed above.

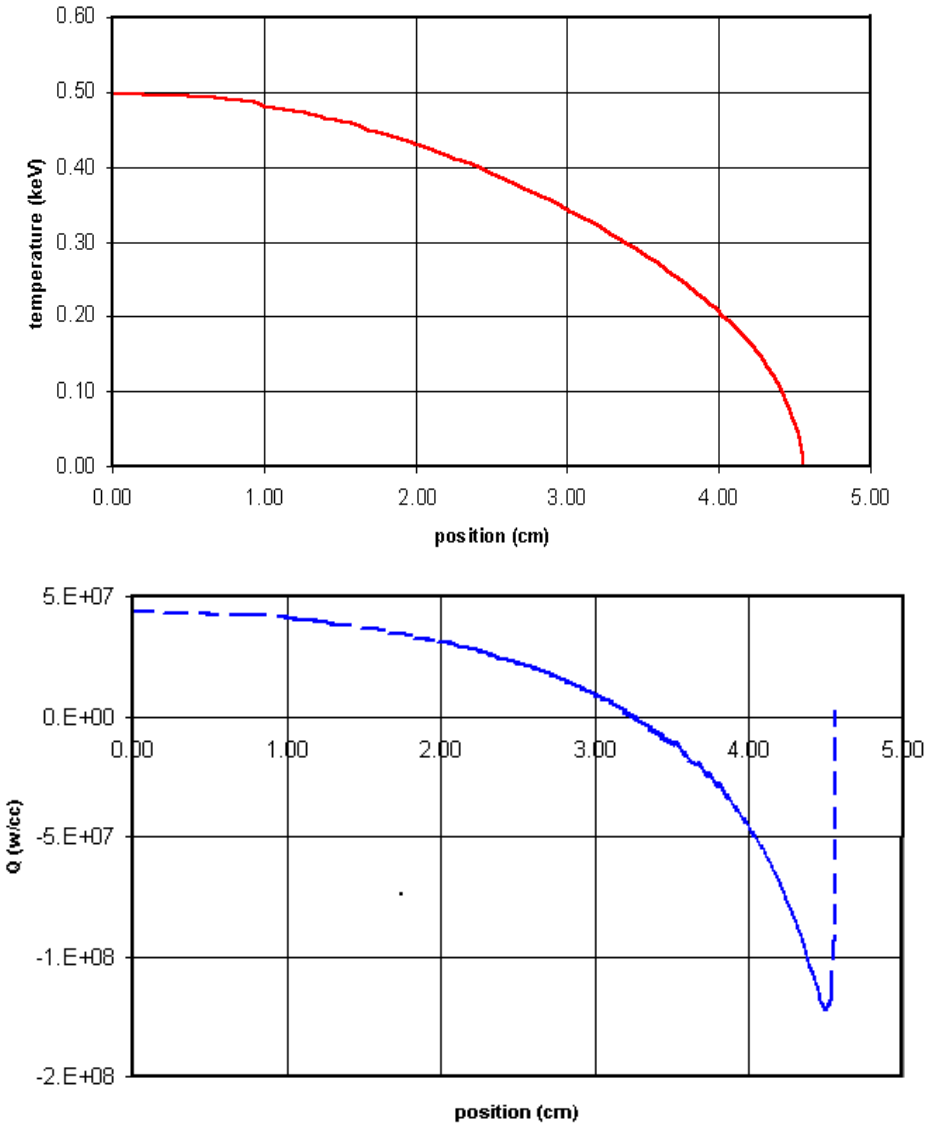

Figure 4. Temperature profile (a) and the associated heating/cooling balance Q (b).

Assuming that bremsstrahlung is the correct spectral type for the plasma emission, we are able to estimate the (rms) average plasma electron density history based on the absolute diode responses. After initially rising to nearly 10^{19} cm-3, the electron density fell to about 10^{18} cm-3 [8]. Until the disruption of the diode filters, both the temperature history and estimated plasma density are very similar to that calculated by the 2-D MHD code MHRDR.

10. STATIONARY WALL-SUPPORTED PLASMAS

We have calculated a 1-D stationary isobaric temperature profiles in a magnetized DT plasma for the case of uniform volumetric heating. One-dimensional slab geometry was necessary in order to utilize some analytic results derived by Ryutov and Fowler [9]. The density profile in an isobaric plasma would be approximately the inverse of the temperature profile. Besides the isobaric assumption, it was assumed that the magnetic field moved with the plasma (i.e., that the electrical conductivity is very high), and that the total pressure was the sum of the magnetic and gas pressures. This meant that as the temperature falls toward zero near the wall, the density remains finite because the flow of the plasma carries the field with it, resulting in an increased magnetic pressure near the wall.

Figure 4 shows a) a representative temperature profile and b) the associated balance between the uniform heating and the energy loss from each layer of plasma in the profile. In the region where the gradient becomes steeper there is net cooling. The case shown is for slab geometry because the analytic expressions simplify the calculations, but a similar profile would exist for the case of cylindrical or spherical symmetry. The solution for such a profile can only exist for a finite wall temperature, for which the lowest value possible depends on the central temperature and density.

For the case of fusion self-heating one would expect three profiles, two stable profiles with an unstable profile between the two stable profiles. If the heating were due to fusion energy production it would not be uniform along the profile, but one would expect a similar steady state profile. Upper and lower stable profiles were calculated in an ignition critical profile study [10]. In that study of an isobaric un-magnetized plasma it was shown that if one is able to establish a plasma temperature profile in the region between the ignition critical profile and the upper stable profile, fusion ignition would occur. We speculate that an ignition critical profile should also exist for magnetized target fusion, but two-dimensional effects necessarily complicate the calculation of such a profile. In addition, because of lower density operation, expansion cooling should be much more important for magnetized target fusion than for inertial confinement fusion.

11. THERMAL STABILITY OF A WALL SUPPORTED PLASMA

In 1978 Lindemuth performed a dynamic calculation using a 2-D MHD code with radiation for the case of an initially uniform magnetized plasma in contact with 1) a thermally insulating, but electrically conducting wall at an inside surface and 2) a cold, thermally conducting wall on the outside [11]. The effects of both electrically conducting and electrically insulating outer walls were calculated. The geometry was cylindrical with an azimuthal magnetic field. The plasma temperature, density, and field profiles evolved from an initially uniform state to produce a gradient near the wall, but the process also developed a radial velocity toward the outer wall that carried field and plasma outward and thereby adjusted the pressure gradient caused by the cooling at the outer wall. For an electrically conducting outer wall, after 20 μs, not only did the plasma acquire a bulk motion toward the wall, but it also developed a convective motion as well. However, because the convection increased the cooling rate and the cooling wave lessened the temperature gradient, it tended to remove the unstable conditions that started the convection.

Lindemuth compared the strictly 1-D case with the 2-D case, which allowed convective motion in the plasma. The plasma thermal energy always far exceeded the kinetic energy. However, by 16 μs there was only half the plasma thermal energy in the 2-D case as there was for the 1-D case, because the convection significantly enhanced cooling to the wall.

However, the reduction in thermal energy was only a factor of about two, which is far from devastating.

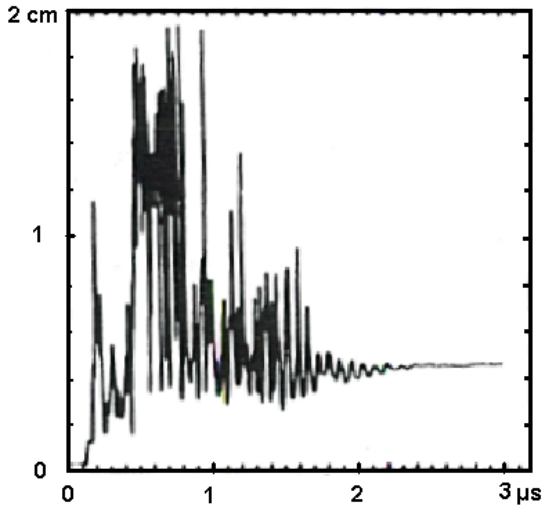

Figure 5. A plot against time of the radius inside of which there is 90% of the Z-pinch current at mid-plane.

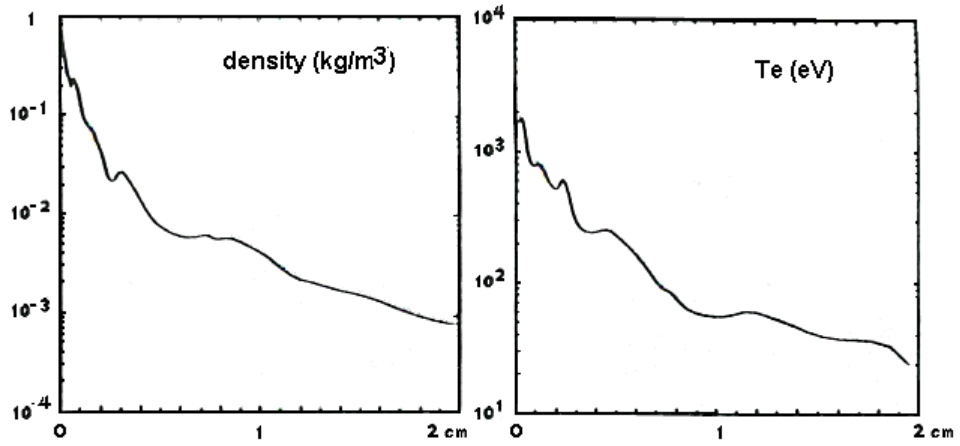

Figure 6. Temperature and density profiles for the Z-pinch plasma at 2.42 μs.

A similar behavior is exhibited for the case of a dense Z-pinch inside a conducting cylinder. In this case the magnetic field tends to provide some degree of confinement for the plasma column, which is m=0 unstable. The instability leads to convective motions, which step-wise evolve the plasma toward a Kadomtsev-like profile. The dense Z-pinch evolution from a highly unstable state toward quasi-stable Kadomtsev-like profile is illustrated in Figure 5, which is a plot against time of the radius inside of which there is 90% of the Z-pinch current at mid-plane. After an early period of wild swings of the 90% radius, it settles toward a steady value. While this case significantly differs from Lindemuth's 1978 calculations, the Z-pinch plasma's time-dependent behavior is similar.

In these Z-pinch calculations the mass-averaged Z-pinch plasma temperature rose to 300 eV in about 2 μs and thereafter remained constant, despite a significant fall-off in the

current supporting the Z-pinch. Late time temperature, density and field profiles are shown in Figure 6.

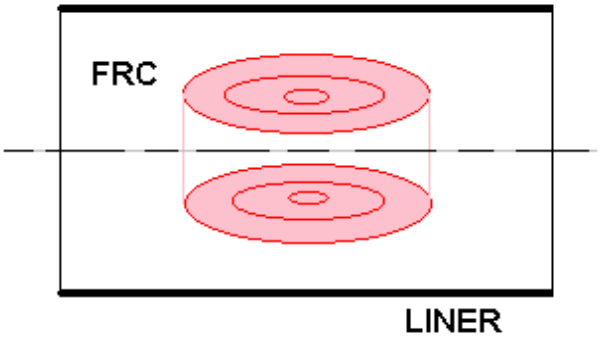

Figure 7. Basic elements of an MTF experiment.

12. AN MTF EXPERIMENT

The basic elements of an MTF experiment are shown in Figure 7. We plan to create a field-reversed configuration (FRC) and translate it into a cylindrical solid liner, which will be magnetically imploded to compress the FRC. An empty liner implosion experiment was done in 1999 using the Shiva-Star capacitor bank at the Air Force Research Lab in Albuquerque[12]. That experiment performed as calculated by a Los Alamos 2-D MHD code. The FRC (theta-pinch) apparatus is currently being built at Los Alamos. We intend to inject the FRC it generates into a similar metal liner with an axial magnetic field. If the apparatus generates a satisfactory FRC and the liner performs as already experimentally demonstrated, we should have the basis for our first MTF proof-of-principle experiment.

We have used the Moqui 2-D MHD code as modified by Milroy at the University of Washington to calculate the performance of the theta-pinch apparatus. Using the appropriate theta-pinch current for the circuit parameters for the capacitor bank and transmission line, we have calculated both stationary and translated FRCs. A cylindrical theta-pinch coil and two cusp coils were used to generate the stationary FRC, but a conical theta-pinch coil was substituted for the cylindrical one to provide a field gradient necessary for translation.

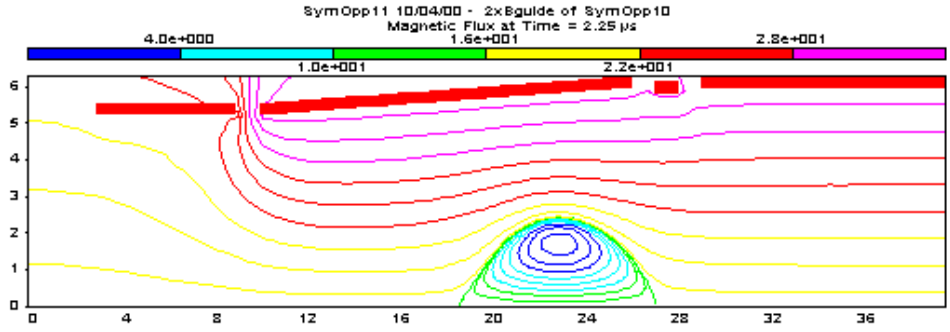

Figure 8. FRC translation has already begun while the conical theta-pinch is still being formed.

Figure 8 shows that the conical theta-pinch begins translation while the FRC is still being formed. For the complete MTF experiment being planned for next year, the translated FRC must enter the liner and remain there long enough to be compressed.

Depending on the way in which the gas is injected into the theta-pinch apparatus before the FRC is formed and upon various Moqui parameters, the FRC may translate different distances into the liner before coming to rest. It will be necessary to calibrate the Moqui code to match the theta-pinch performance in order to make more definite predictions regarding the translation of the FRC.

We also modified the translation calculation to look at a symmetric plasma injection into the liner. This modified calculation used a mirror boundary inside the simulated liner, so that two FRCs collide and merge. Soon after formation, the calculated FRC temperatures reached about 300 eV and then began to relax toward similar electron and ion temperatures. However, the plasma lost mass faster than energy, so that the electron temperature began to rise, and at late time the electrons were far out of equilibrium with the ions.

Numerical experiments were done in which the viscosity and density of the plasma were changed. The dynamics of the FRC depended strongly on the density of the gas through which the FRC had to pass to move inside the cylindrical liner. Viscosity mattered only a little. However, viscosity and conductivity do effect the ability of Moqui to carry a calculation to completion during the merging of two oppositely directed FRCs. Currently, Moqui can provide only a qualitative prediction of the FRC behavior. By adjusting some of the parameters in the code to bring it into quantitative agreement with the experiment, we hope to make it a better predictive tool.

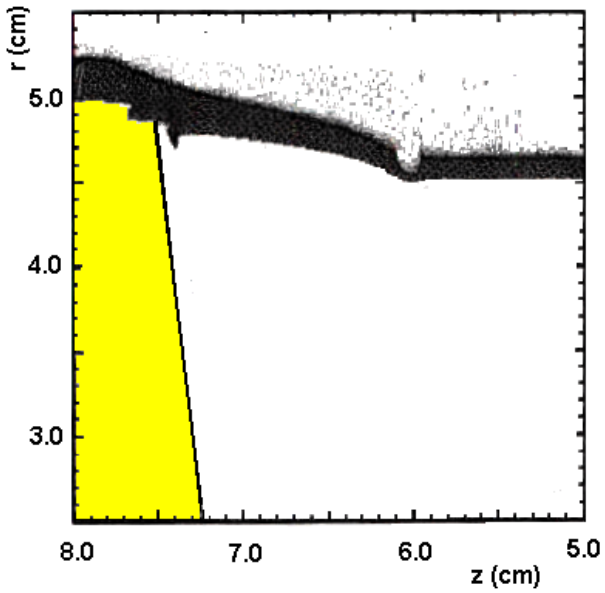

Figure 9. Failure of a tapered liner that was thickened near one electrode.

13. LINER DESIGNS

Another way of insuring that the FRC does not leave the liner before it is compressed is to design a liner that closes before the FRC can leave. One way to do this is to taper the liner or vary its thickness. Los Alamos has performed detailed calculations of the performance of an empty solid liner. It is important to understand why various problems occur in solid liner implosions and to develop the capability to design liners for special applications. A detailed account of a liner experiment done on the Shiva-Star capacitor bank appears elsewhere in these proceedings [12]. In part, the success of that experiment attests to the quantitative MHD predictive capability currently in place for liner design.

In the liner calculations reported here, the liner was driven by a current from an external circuit with parameters appropriate for the Shiva-Star capacitor bank at AFRL in Albuquerque. Calculations were done for a straight liner with a uniform thickness and for another that was tapered near each electrode. Since each problem was symmetric about the mid-plane, only half the liner was included for each calculation. Both liners were empty. The straight liner performed well when the appropriate electrode angle was used. It made a smooth transition from electrical connection through the liner around the electrodes to a sliding contact. However, the tapered liner ruptured due to the discontinuity where the taper ends. This happened very early, as shown in Figure 9. It appears that the tapered part of the liner had enough strength to resist the electromotive force due to the Z-directed

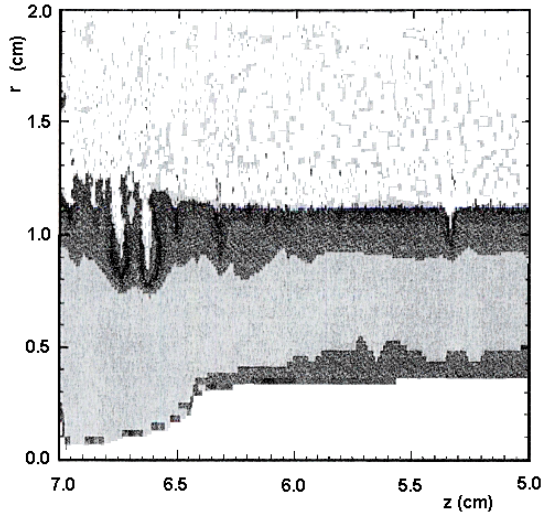

Figure 10. State of the straight liner near the radius of greatest convergence (4mm). The shading indicates the variation of densities within the liner.

current in the liner, but the straight section moved more quickly due to its lower areal density. This added to the stress in the region where the taper ended, which was where the rupture was initiated. Figure 10 shows that the straight liner maintained its continuity all the way down to the radius of greatest convergence (4mm). Even inside 5 mm radius with a convergence greater than 10, the central part of the straight liner remained straight.

14. CONCLUSION

MTF does not require a very powerful driver. Adequate pulsed power drivers for MTF experiments already exist, so that the initial development of MTF should be rapid, even with a modest (but adequate) expenditure. Thus far, funding has not been adequate.

Because pulsed power drivers are much more efficient than lasers, high gain targets should not be necessary for an economical fusion based power plant. The MAGO apparatus appears to be capable of providing a satisfactory target plasma, but because of diagnostic failure a few microseconds after the first plasma emission was seen in one well-diagnosed experiments [8], we have no firm proof that it lasts long enough for a successful compression experiment.

Los Alamos is exploring an alternative target plasma. This takes the form of an FRC, which can be translated into a solid liner for compression. The intention of the compression experiment would be to provide a limited proof of principle. We performed a successful

empty-liner experiment last year, so that part of the experiment is ready. However, we are still in the process of building a theta-pinch to generate a FRC.

Although the existing computational capability has been employed to the greatest advantage, there is a need for improved and expanded capabilities. For example, the Moqui code is qualitatively predictive, but accurate design requires quantitative predictions. Also, in the past we have been forced to use explicit MHD codes, and numerical stability forces excessively short time steps, resulting in excessive run times. In addition, some anticipated computational problems would demand expanded physics capabilities. Therefore, an expanded theoretical/computational capability will be essential for continued progress in understanding MTF.

If proven to be a viable approach to fusion, MTF may have applications for energy production, space propulsion, and as an intense neutron source for medical isotope production. Pulsed neutron sources avoid build-up of many unwanted isotopes that occur when a fission reactor is used for isotope or energy production. During the early stages, all of these potential applications could share a single development path.

We are making progress toward understanding MTF, but available resources currently limit the rate of progress. No major new pulsed power facilities are needed to reach this near-term goal. Much work remains, but adequate funding is essential, if the potential benefit of MTF is to be realized.

REFERENCES

1. R.C. Kirkpatrick and G. Idzorek, Proceedings of the Seventh International Conference on Megagauss Magnetic Field Generation (MG-VII), Sarov, Russia (1996).
2. I.R. Lindemuth and M.M. Widner, Phys. Fluids **24**, 753 (1981)
3. M.A. Sweeney and A. Farnsworth, Nucl. Fusion **21**, 41 (1981)
4. I.R. Lindemuth and R.C. Kirkpatrick, Nucl. Fusion **23**, 263 (1983).
5. D.P. Kilcrease and R.C. Kirkpatrick, Nuclear Fusion **28**, 1465 (1988)..
6. J.D. Lindl, in ICF Course & Workshop (Varenna, Italy, 1988), A. Caruso & E. Sindoni, Ed.
7. R.C. Kirkpatrick, I.R. Lindemuth, R.E. Reinovsky, and P.T. Sheehey, Current Trends in International Fusion Research, Proceedings, Edited by Emilio Panarella, Plenum Press, New York, 1997.
8. R.C. Kirkpatrick and I.R. Lindemuth, Current Trends in International Fusion Research, Proceedings of the Second Symposium, Edited by Emilio Panarella, NRC Research Press, National Research Council of Canada, Ottawa, ON K1A 0R6 Canada,1999.
9. D. Ryutov, notes (1998) and K. Fowler, discussions at Los Alamos (1998).
10. R.C. Kirkpatrick, Nuclear Fusion **21**, 1457 (1982).
11. I.R. Lindemuth, Physics of Fluids **21**, 1723 (1978)
12. J.H. Degnan, T. Cavazos, S.K. Coffey, et al., Current Trends in International Fusion Research, Proceedings of the Fourth Symposium, Edited by Charles D. Orth, Emilio Panarella, and Richard F. Post, NRC Research Press, National Research Council of Canada, Ottawa, ON K1A 0R6 Canada, 2001.